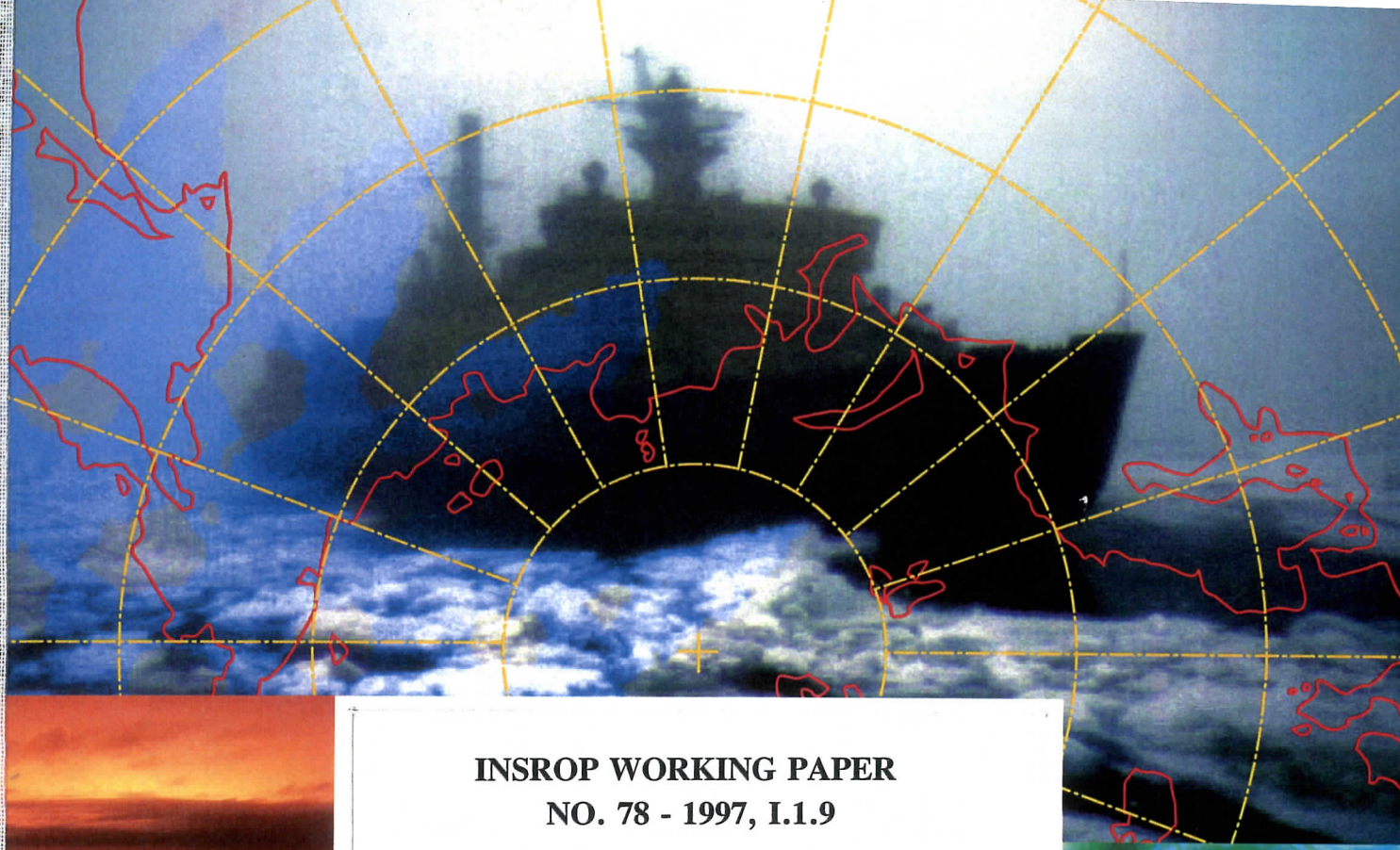

INSROP WORKING PAPER
NO. 78 - 1997, I.1.9

Experimental Study to Separate into Components the Interaction Force between Propeller and Ice Piece

By Kenkichi Tamura and Hajime Yamaguchi

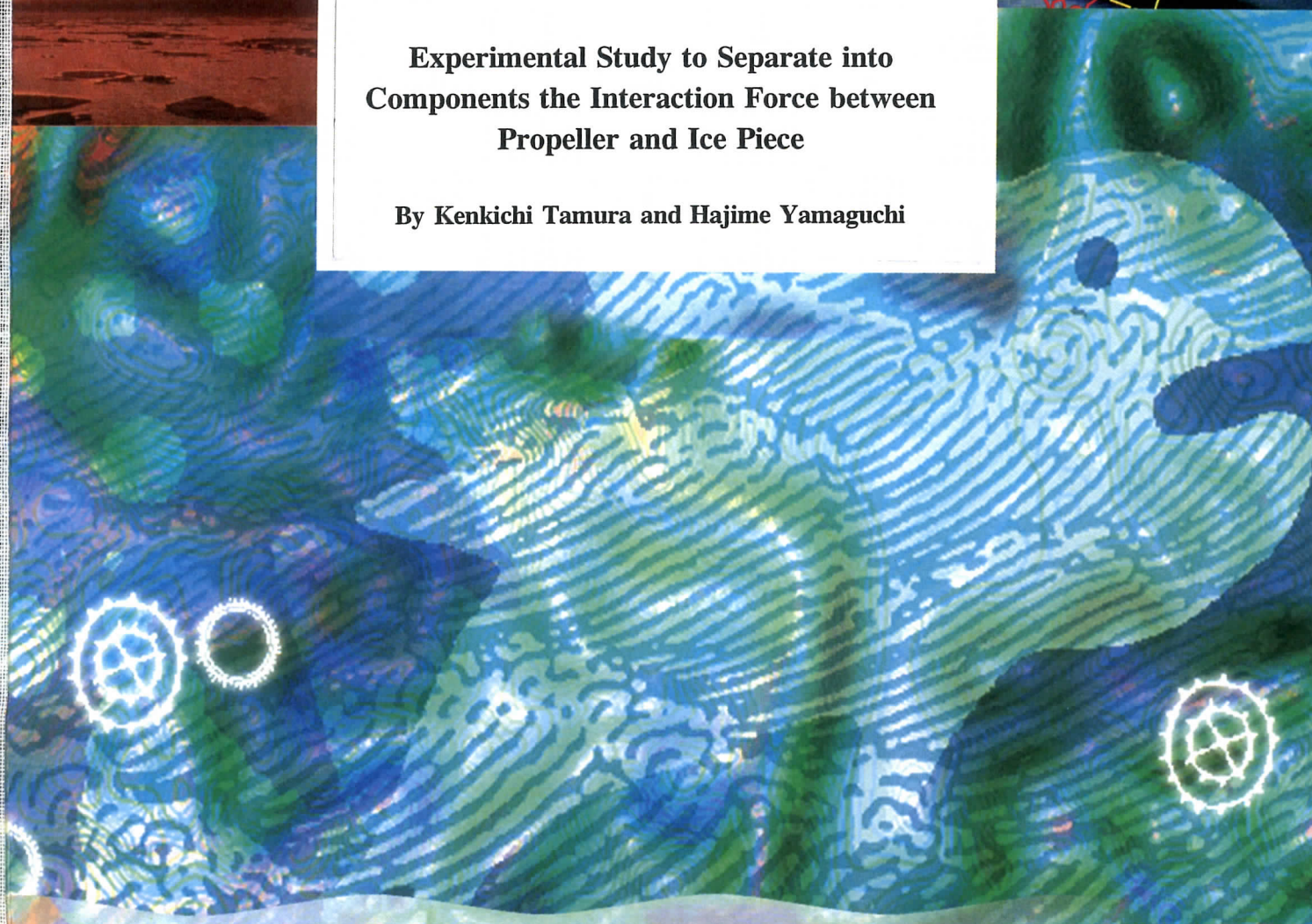

INSROP International Northern Sea Route Programme

Central Marine Research & Design Institute, Russia

The Fridtjof Nansen Institute, Norway

Ship and Ocean Foundation, Japan

International Northern Sea Route Programme (INSROP)

Central Marine Research & Design Institute, Russia

The Fridtjof Nansen Institute, Norway

Ship & Ocean Foundation, Japan

INSROP WORKING PAPER NO. 78-1997

Sub-programme I:	Natural Conditions and Ice Navigation
Project I.1.9:	Hydrodynamic Aspects on Ice/Propeller Interaction
Supervisor:	Hajime Yamaguchi
Title:	**Experimental Study to Separate into Components the Interaction Force between Propeller and Ice Piece**
Authors:	**Kenkichi Tamura (1) and Hajime Yamaguchi (2)**
Addresses:	(1) Arctic Vessel and Low Temperature Engineering Division, Ship Research Institute, Ministry of Transport, 6-38-1 Shinkawa, Mitaka-shi, Tokyo 181, JAPAN. (2) Department of Naval Architecture and Ocean Engineering, Graduate School of Engineering, University of Tokyo, 7-3-1 Hongo, Bunkyo-ku, Tokyo 113, JAPAN
Date:	5 May 1997
Reviewed by:	Dr. Stephen J. Jones and Dr. Brian Veitch, Institute for Marine Dynamics, National Research Council Canada, St.John's, Newfoundland, CANADA.

What is an INSROP Working Paper and how to handle it:

This publication forms part of a Working Paper series from the **International Northern Sea Route Programme - INSROP**. This Working Paper has been evaluated by a reviewer and can be circulated for comments both within and outside the INSROP team, as well as be published in parallel by the researching institution. A Working Paper will in some cases be the final documentation of a technical part of a project, and it can also sometimes be published as part of a more comprehensive INSROP Report. For any comments, please contact the authors of this Working Paper.

FOREWORD - INSROP WORKING PAPER

INSROP is a five-year multidisciplinary and multilateral research programme, the main phase of which commenced in June 1993. The three principal cooperating partners are **Central Marine Research & Design Institute (CNIIMF)**, St. Petersburg, Russia; **Ship and Ocean Foundation (SOF)**, Tokyo, Japan; and **Fridtjof Nansen Institute (FNI)**, Lysaker, Norway. The INSROP Secretariat is shared between CNIIMF and FNI and is located at FNI.

INSROP is split into four main projects: 1) Natural Conditions and Ice Navigation; 2) Environmental Factors; 3) Trade and Commercial Shipping Aspects of the NSR; and 4) Political, Legal and Strategic Factors. The aim of INSROP is to build up a knowledge base adequate to provide a foundation for long-term planning and decision-making by state agencies as well as private companies etc., for purposes of promoting rational decisionmaking concerning the use of the Northern Sea Route for transit and regional development.

INSROP is a direct result of the normalization of the international situation and the Murmansk initiatives of the former Soviet Union in 1987, when the readiness of the USSR to open the NSR for international shipping was officially declared. The Murmansk Initiatives enabled the continuation, expansion and intensification of traditional collaboration between the states in the Arctic, including safety and efficiency of shipping. Russia, being the successor state to the USSR, supports the Murmansk Initiatives. The initiatives stimulated contact and cooperation between CNIIMF and FNI in 1988 and resulted in a pilot study of the NSR in 1991. In 1992 SOF entered INSROP as a third partner on an equal basis with CNIIMF and FNI.

The complete series of publications may be obtained from the Fridtjof Nansen Institute.

SPONSORS FOR INSROP

- Nippon Foundation/Ship & Ocean Foundation, Japan
- The Government of the Russian Federation
- The Norwegian Research Council
- The Norwegian Ministry of Foreign Affairs
- The Norwegian Ministry of Industry and Trade
- The Norwegian Ministry of the Environment
- State Industry and Regional Development Fund, Norway
- Norsk Hydro
- Norwegian Federation of Shipowners
- Fridtjof Nansen Institute
- Kværner a.s.
- Phillips Petroleum Company Norway

PROFESSIONAL ORGANISATIONS PERMANENTLY ATTACHED TO INSROP

- Ship & Ocean Foundation, Japan
- Central Marine Research & Design Institute, Russia
- Fridtjof Nansen Institute, Norway
- National Institute of Polar Research, Japan
- Ship Research Institute, Japan
- Murmansk Shipping Company, Russia
- Northern Sea Route Administration, Russia
- Arctic & Antarctic Research Institute, Russia
- ARTEC, Norway
- Norwegian Polar Research Institute
- Norwegian School of Economics and Business Administration
- SINTEF (Foundation for Scientific and Industrial Research - Civil and Environmental Engineering), Norway.

PROGRAMME COORDINATORS

- **Yury Ivanov, CNIIMF**
  Kavalergardskaya Str.6
  St. Petersburg 193015, Russia
  Tel: 7 812 271 5633
  Fax: 7 812 274 3864
  Telex: 12 14 58 CNIMF SU
- **Willy Østreng, FNI**
  P.O. Box 326
  N-1324 Lysaker, Norway
  Tel: 47 67 11 19 00
  Fax: 47 67 11 19 10
  E-mail: sentralbord@fni.no
- **Ken-ichi Maruyama, SOF**
  Senpaku Shinko Building
  15-16 Toranomon 1-chome
  Minato-ku, Tokyo 105, Japan
  Tel: 81 3 3502 2371
  Fax: 81 3 3502 2033
  Telex: J 23704

Project I.1.9*

Experimental Study to Separate into Components the Interaction Force between Propeller and Ice Piece

by

Mr. Kenkichi Tamura
Arctic Vessel and Low Temperature Engineering Division
Ship Research Institute, Ministry of Transport
6-38-1 Shinkawa, Mitaka-shi, Tokyo 181, JAPAN
Phone:+81-422-41-3155
Fax:+81-422-41-3152
E-mail: *tamura@srimot.go.jp*

and

Prof. Hajime Yamaguchi (Supervisor)
Department of Naval Architecture and Ocean Engineering
Graduate School of Engineering
University of Tokyo
7-3-1 Hongo, Bunkyo-ku, Tokyo 113, JAPAN
Phone: +81-3-3812-2111 ext.6536
Fax: +81-3-3815-8360
E-mail: *yama@fluidlab.naoe.t.u-tokyo.ac.jp*

---

* The name of the project is "Hydrodynamic Aspects in Ice/Propeller Interaction". This report contains more works than were executed in the INSROP Project I.1.9, in order to provide the comprehensive understanding of the problem.

ABSTRACT

When an ice piece collides with a propeller, it leads to an impact load on the propeller blade, causing damage to the propeller blade and/or engine trouble. So far, the impact load has been treated from the aspect of ice breakage only. It is presumed, however, that other factors, such as hydrodynamic force and inertia force of the ice piece, also affect this phenomenon. The importance of these forces has recently been investigated and reported. The shallow water along parts of the Northern Sea Route requires a shallow draft ship, resulting in more frequent interaction between the propeller and ice pieces. Also, the limited propeller diameter due to the shallow draft leads to greater load on the propeller. A nozzle propeller has some advantages over the conventional open propeller in such conditions.

Taking the above issues into consideration, our study deals with ice interaction with a nozzle propeller. Ice impact load is divided into 4 components: force due to ice failure, force due to momentum change of an ice mass, force due to the added mass of ice, and hydrodynamic force due to proximity and flow distortion between the propeller blade and ice. This paper describes the experiments on the division of the force into these four components. An ice collision test in water contains all of the force components. An ice blockage test in water, where an ice block is placed in front of the propeller without touching the propeller blade, yields the hydrodynamic force. An ice collision test in air yields the ice failure force and the inertia force due to the ice mass only. Finally, an ice collision test with ice of various strengths reveals the effects of ice strength.

A nozzle propeller model of a 267mm-diameter propeller was used in these experiments. The thrust, torque and spindle torque of one blade were measured and analyzed for all four experiments described above. The following results were obtained:

1. The ice failure force component seems to be proportional to the ice strength.
2. For the thrust, the inertia force is by far the major component and the ice failure force is minor. The hydrodynamic force increases the thrust, while the other forces decrease it.
3. For the torque, the ice failure force is strongly dependent on the ice strength and is the largest of all the force components, followed by the hydrodynamic force and then the inertia force which is about half the hydrodynamic force.
4. For the spindle torque, the inertia force and the ice failure force are the largest components and are comparable to each other. Hydrodynamic force is approximately half the inertia force.

As mentioned above, inertia and hydrodynamic forces are comparable to or larger than the ice failure force. Rational scaling laws must be considered and applied to the respective force components when ice forces on a full-scale propeller are extrapolated from the results of the model experiments.

1 INTRODUCTION

Ice-propeller interaction is one of the major issues which should be taken into consideration for the safety of a ship in ice. There have been a number of reported accidents in which propellers were damaged by ice. Many ice-going vessels carry spare blades to case of such accidents. Ice loads on the propeller could even lead to shafting and engine failures.

There are two different approaches for treating the problem from a practical point of view. The first approach is the prevention of the ice-propeller interaction. One of the most important issues in the design of ice-going vessels is protecting the propellers from ice. Not only the stern form and propeller location, but ship's other features such as the ice foot, rise of the floor and side flare are important for less interaction with ice. Ship operation is also important for the prevention of ice-propeller interaction. Propellers are especially vulnerable during sternward operations. The second approach is the estimation of loads on a propeller due to interaction with ice. Some criteria on the load due to ice-propeller interaction should be given in the structural design of the propulsion system, including propellers, shafting, gears and engine.

From the viewpoint of ice-propeller interaction, geographical features on the Northern Sea Route (NSR) give an unfavorable condition for a ship. Due to the shallow water of some areas and ports on the NSR, ships sailing along the route must have a shallow draft, which results in a high possibility of ice-propeller interaction. Realizing the value of a study of ice-propeller interaction in NSR vessels, a research project was commenced on the ice-propeller interaction problem (Kitagawa, 1996; Tamura and Yamaguchi, 1996). This project focuses on the loads on the propeller due to interaction with ice, i.e. the second of the two approaches mentioned above.

In this paper, we describe the ice-propeller interaction project. A model propeller was designed and manufactured in 1994. In 1995, the propeller was remodelled for the installation of sensors to measure the forces on a blade. Model tests were performed in the ice tank and towing tank of the Ship Research Institute, Japan (SRIJ). We present some experimental results and the first attempt to divide the ice-propeller interaction force into its components.

2 SCENARIO OF ICE-PROPELLER INTERACTION AND ICE LOAD COMPONENTS

2.1 Ice Load Components

Ice-propeller interaction is a very complicated problem, and has many factors which should be taken into account in the study of the problem. Jagodkin (1963) proposed a model to estimate the torque of a propeller interacting with ice, and several models were subsequently proposed (Jussila and Soininen, 1991). Most of them assumed the milling situation, so the load required

to mill an ice block was taken into account. Based on these classic models, shaft torque due to ice-propeller interaction was calculated and compared with mainly full-scale data. Veitch (1995) and Koskinen et al. (1996) recently developed elegant numerical simulation methods where the collision between an ice block and propeller blade is treated in a more general and sophisticated manner. However, studies on nozzle propellers are rather limited, and it is considered that the scenario of ice interaction with a nozzle propeller is somewhat different from that with an open propeller since the size of ice blocks colliding with propeller blades is restricted by the nozzle.

Recently, a joint research project between Canada and Finland was carried out on ice-propeller interaction (Fleet Technologies Ltd., 1992; Shih and Zheng, 1992; Soininen and Veitch, 1996; Walker et al., 1994; Walker and Bose, 1994). Their results suggested that noncontact loads, defined as the loads on the propeller blades due to interruption of the hydrodynamic flow by an ice block close to the propeller, are important. Here, loads due to the breaking of ice are defined as contact loads. The experiments and calculations of the joint research have shown that the noncontact load may, under some conditions, be as large as the contact load. Based on this result, a new project was commenced to gain further understanding of the hydrodynamic aspects of the problem both numerically (Bose, 1995) and experimentally (Walker et al., 1997).

Results of the joint Canadian Finnish research project have shown that it is important to have a comprehensive scenario for load placement on the propeller. One of the objectives of the present study is to establish the scenario based on experiments using models, while the numerical approach has been undertaken by Veitch et al. (1997), who are trying to couple hydrodynamic and ice contact computations. As the starting point of this experimental study, the following equation is proposed for the total load on a propeller blade interacting with ice:

$$F_{total} = F_{ice} + F_{hydro} + F_{inertia1} + F_{inertia2}, \qquad (1)$$

where F_{total} is the total load on a blade. Figure 1 schematically illustrates each load component.

(1) F_{ice}

F_{ice} is the load applied during breakage of an ice block and should be treated with the fracture mechanics. There will be two modes of ice breakage. When the ice block is large or the ice block is stuck between the hull and propeller, the propeller blade will intrude into the ice block, as is the case in the classic ice milling theories. The load

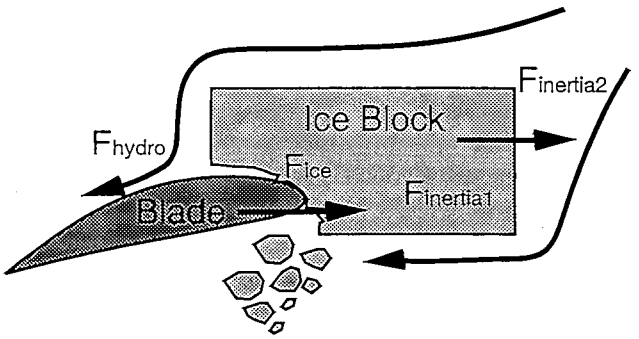

Fig. 1 Load Components on a Propeller Blade

to cut the ice will be affected by factors such as compressive and shear strengths of ice, cutting depth and interaction speed. Such milling, however, would be rare for a nozzle propeller. When the ice block is small or in case of nozzle propeller, the ice will collide with the propeller blade and will be crushed into pieces. The load will be influenced by factors such as volume of crushed block and crushing strength of ice.

(2) F_{hydro}

This is the hydrodynamic load due to the presence of ice. This load is similar to the noncontact force investigated by the joint Canadian Finish research project. The presence of an ice block leads to flow restriction and flow separation from the edge of the block. In the narrow gap between ice block and blade, the flow is locally accelerated, resulting in increase of the blade force. The load increases rapidly as the ice block approaches the blade.

(3) $F_{inertia1}$

This is the load due to inertia of total ice mass including crushed ice pieces. When an ice block contacts a propeller blade, a momentum is given to the ice, and a blade receives a reaction.

(4) $F_{inertia2}$

This is the load due to inertia of added mass of ice. An added mass is caused by movement of ice block and broken ice pieces in water.

Since ice with higher strength can be more accelerated when impacted by a blade, inertia forces, $F_{inertia1}$ and $F_{inertia2}$, should be dependent on the ice strength as well as F_{ice}. It is unknown, however, how much the effects of ice strength are. In order to verify this, we observed the ice motion during ice-propeller contact using a high speed video for various ice strengths. There was no significant effect of ice strength on ice movement, such as ice acceleration and travel distance. It can be considered, therefore, that the effects of ice strength on $F_{inertia1}$ and $F_{inertia2}$ are negligible at least within the range of the present experiments.

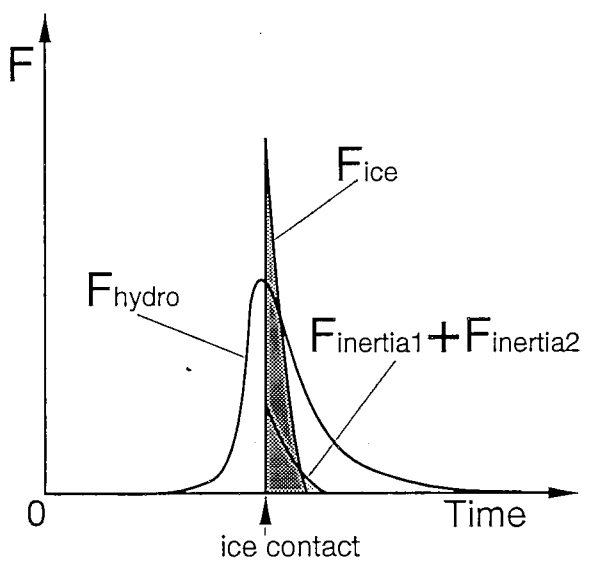

Fig. 2 Schematic Time History of Each Load Component

Figure 2 schematically shows time histories of the load components defined above. F_{ice}, $F_{inertia1}$ and $F_{inertia2}$ have sharp peaks at the moment of contact. F_{hydro} also reaches its peak near the moment of contact, but its skirt is wider compared to those of the other loads. In this study, the ice load will be decomposed using peak values of the experiments described in the next section. It is probable that the peak of F_{hydro} appears slightly before the contact. However, the error due to this time difference will not be significant since the time variation curve of F_{hydro} is gentle particularly near the peak.

For quantitative understanding of ice-propeller interaction, it is necessary to know each load component. For this purpose, separation of the components is required. In this study, experimental separation of load components is attempted.

2.2 Experimental Decomposition Method

To decompose the above-mentioned four ice force components, the following experiments were planned and executed in the ice tank of the Ship Research Institute, Japan (SRIJ).

Ice Block Collision Test in Water. In this test ice blocks are fed into a propeller operated in the water. Figure 3 shows the experimental setup for this test. An ice feeder, which is like a slide, is set on a subcarriage connected to the main carriage of ice tank. The ice blocks are pushed down along the slide and collide with the propeller at constant time intervals. This is the basic experiment of ice-propeller interaction, and the results include all the ice load components.

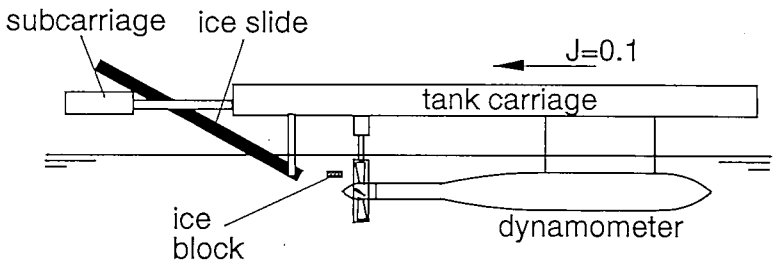

Fig. 3 Experimental Setup for Ice Block Collision Test in Water

Ice Block Collision Test in Air. The procedure for this test is the same as that for the test in water, except that test is performed in air instead of water. The size of ice blocks and revolution speed of the propeller are the same as those in the test in water. The result of this test does not include the inertia of added mass, $F_{inertia2}$, or the hydrodynamic load due to the presence of ice, F_{hydro}.

Ice Blockage Test in Water. This is a test for the direct measurement of hydrodynamic load due to the presence of an ice block. Figure 4 shows the arrangement for this experiment. In this test, an ice block is placed in front of the propeller in operation. The ice block gradually approaches the propeller until it touches the propeller blades. Loads on the propeller are measured as a function of the distance between the propeller and the ice block. This result includes only hydrodynamic load due to the presence of ice, F_{hydro}.

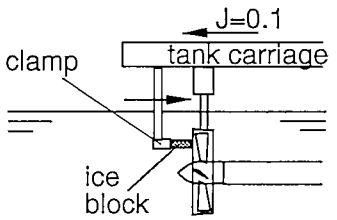

Fig. 4 Arrangement for Blockage Test

Ice Block Collision Test in Water and Air Using Ice Blocks of Various Strength.

Table 1 summarizes the force components included in the above-mentioned experiments. F_{hydro} and $F_{inertia2}$ can be determined by comparing the results of ice collision tests in water and air. F_{hydro} can be determined from the ice blockage test. F_{ice} and $F_{inertia1}$ are separated using the results of tests in air with various ice strengths. As previously mentioned, F_{ice} is a function of ice strength, while the others are not. Thus the zero intersect of the ice force corresponds to $F_{inertia1}$. Figure 5 shows the variation of ice force components in the present decomposition method. As such, all four ice components can be decomposed, at least to a first approximation.

Table 1 Ice Load Components Determinable by Various Tests

	F_{ice}	F_{hydro}	$F_{inertia1}$	$F_{inertia2}$
Ice Contact Test in Water	○	○	○	○
Ice Contact Test in Air	○		○	
Ice Blockage Test in Water		○		
Test in Water with Various Ice Strength	○*	○	○	○
Test in Air with Various Ice Strength	○*		○	

* variable

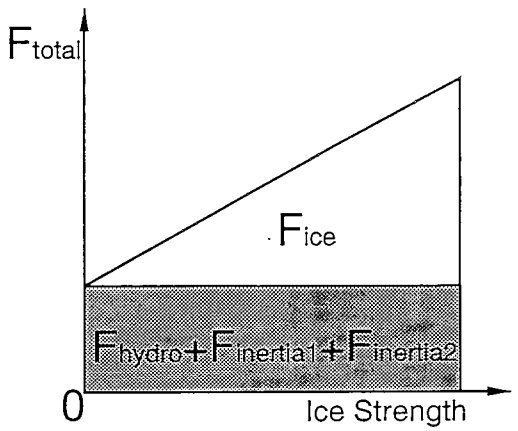

Fig. 5 Variation of Ice Force Components with Ice Strength

3 EXPERIMENT

3.1 Experimental Apparatus

A model of a nozzle propeller was designed and manufactured to be used for experiments in the ice tank. Table 2 and Figure 6 show the design characteristics of the model propeller and nozzle. The model was designed in accordance with the conceptional design of the nozzle propeller for the NSR cargo ship made by the NSR Research Panel in Japan in 1993 (Ishikawa and Kawasaki, 1996; Izumiyama and Uto, 1996; Kishi and Narita, 1996). The scale of the model is 1/18, which is twice as large as the propeller used at a model in the R&D project of the NSR cargo ship. To measure the pressure, bending moment and spindle torque of a blade, the propeller is equipped with sensors, as shown in Table 3 and Fig. 7. On the back of the blade, two Helmholtz cavities with a 0.5-mm-diameter hole are drilled, and a pressure gauge is placed in each chamber behind the hole. To measure the bending moment of a blade, three-axes strain gauges are installed. In total, 12 sensors are installed on the propeller. The pressure gauge on blade C, the strain gauge at the position of r/R = 0.45 on blade C, and the spindle torque strain gauge are used in the present experiment. The nozzle is made of transparent acrylic resin so that the ice-propeller interaction can be observed. The clearance between propeller the tip and nozzle is 2.67 mm.

Table 2 Principal Particulars of Model Propeller

Model Propeller	
Type	CPP
Diameter (mm)	266.66
Pitch Ratio (const)	1.0896
Expand Area Ratio	0.5526
Boss Ratio	0.3810
t/R	0.0776 at r/R=0.381
Rake Angle	0°
Skew Angle	0°
Blade Number	4
Blade Section	MD
Material	BS

Nozzle	
Inner Diameter (mm)	272.0
Outer Diameter (mm)	328.4
Nozzle Length (mm)	133.33
Nozzle Section	Ka4-70 screw series no.19A
Material	Acrylic Acid Resin

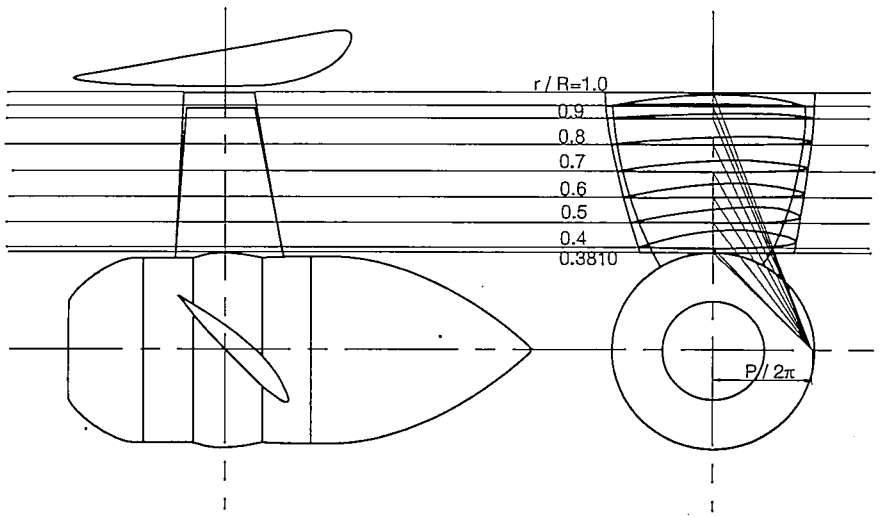

Fig. 6 Model Propeller

Figure 8 shows the block diagram for the experiment in the ice tank. A dynamometer is

Table 3 Gauges on Propeller Blades

Pressure Gauge			
Blade	r/R	Chord	Remarks
B	0.80	50%	Sub (Back)
C	0.70	50%	Main (Back)
Strain Gauge for Bending Moment			
Blade	r/R	Chord	Remarks
C	0.45	50%	(Face)
B	0.50	50%	(Face)
C	0.55	50%	(Face)
Strain Gauge for Spindle Torque			
Blade	r/R	Chord	Remarks
A	-	-	(Boss)

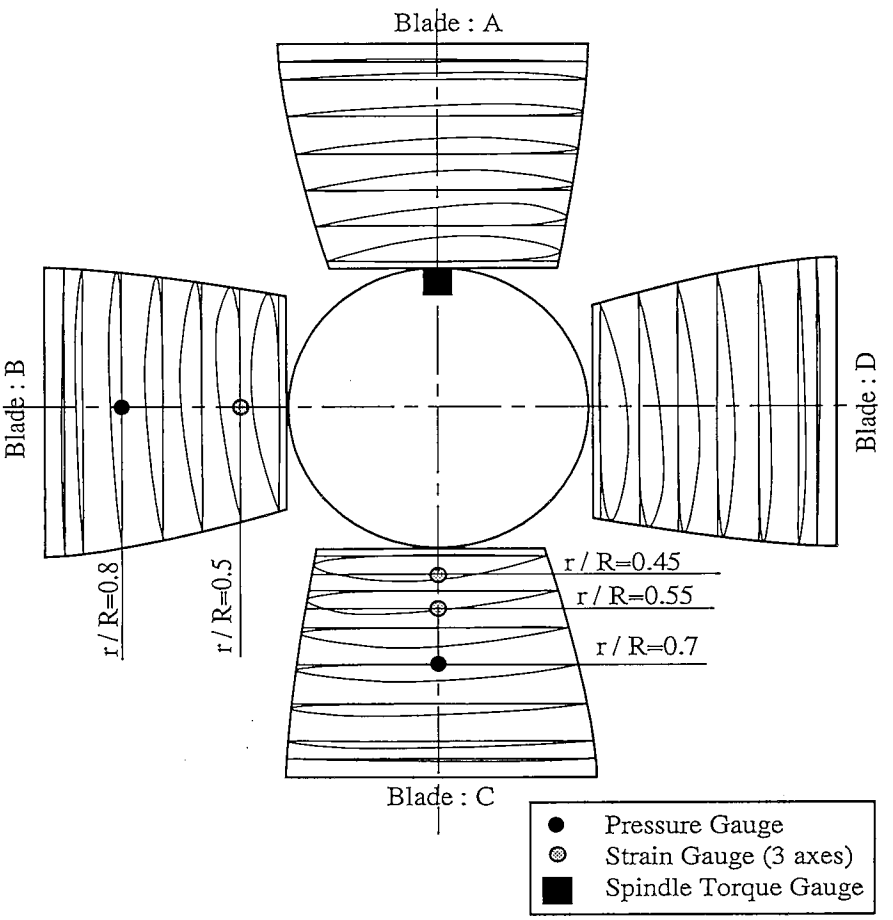

Fig. 7 Gauge Positions on Propeller Blade

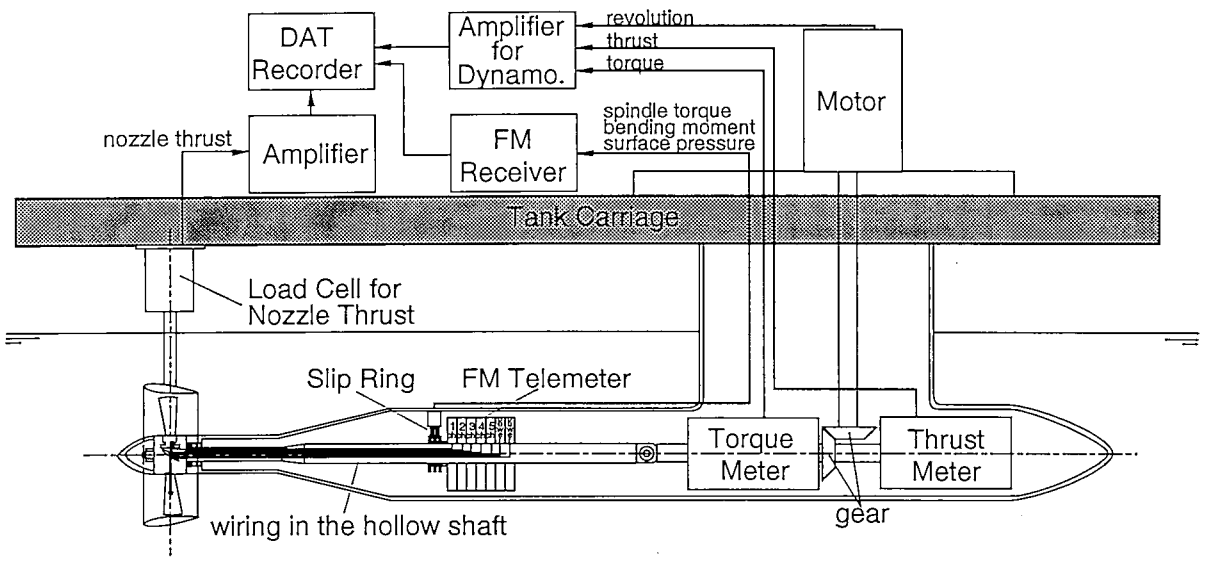

Fig. 8 Propeller Dynamometer and Measurement System

mounted on the tank carriage. Propeller immersion depth can be adjusted by changing the vertical position of the dynamometer. The propeller is driven by a DC motor and has a maximum shaft revolution of 40 rps. Measuring capacities of the dynamometer are 600 N for thrust and 20 Nm for torque, which are high enough to measure the ice contact load. The resonance frequency of the system is over 1 kHz, which is high enough for the present unsteady measurements. The signals from the sensors on the propeller are collected by FM telemeters and sent to the FM receiver via slip rings. The FM transmitter has five channels on which to transmit data. The usual selection of data channels is pressure on the blade (1 channel), bending moment of the blade (3 channels) and spindle torque (1 channel). The maximum frequency of FM telemeters is 2 kHz. The nozzle is connected to the carriage via a two-component load cell to measure nozzle thrust. Measured data are recorded by a DAT data recorder. A high-speed video camera (made by Houei: ACCEL AAA-240, 240 frames/s) is used to record the interaction phenomena. In all tests, the propeller revolution speed is so slow at 4 rps that the blade moves 6 deg per frame of the high-speed video. From the video images, interaction of the ice with the blade can be observed and the contact point can be determined.

3.2 Experimental Condition

Ice block collision tests in water and blockage tests were performed in the SRIJ ice tank (water temperature = -0.1 - -0.2 deg.C), and ice block collision tests in air were performed at a trimming tank room (room temperature = 0 - 1 deg.C) in the ice tank. All ice blocks were made in another small ice tank. The model ice was made of water doped with propylene glycol.

Compressive strength of the ice block ranged from 120 kPa to 1260 kPa. Ice blocks were 100 mm × 100 mm × 30 mm (M-size) and 100 mm × 200 mm × 30 mm (L-size). The shaft torque and thrust, blade bending moment, spindle toque, pressure on the blade and thrust of the nozzle were measured. The propeller revolution speed was 4 rps and the carriage speed was 0.1 m/s, which corresponded to the propeller advance ratio of J=0.1. This advance ratio was determined from the model tests carried out in the R&D project of the NSR cargo ship (Ishikawa and Kawasaki, 1996; Izumiyama and Uto, 1996; Kishi and Narita, 1996).

4 TEST RESULTS

4.1 Ice Block Collision Test in Water

Tests were conducted using 95 ice blocks with various ice strengths. Among them, 23 blocks were L-size.

Figure 9 shows an example of time histories of measured thrust, torque and spindle torque, where thrust and torque are shown in nondimensional form, K_T and $10\times K_Q$, respectively. In this case, an ice block collided with the leading edge of blade A, which was equipped with a spindle torque gauge. The contact position was determined from the high-speed video image. The two peaks before and after the highest peak are due to the contact (or hydrodynamic effect due to proximity) of the ice block with the adjacent two blades. The highest torque peak occurred when the ice block came into contact with the propeller blade A. Thrust and spindle torque peaks appeared slightly before and after the direct contact, respectively. The peak values, defined in the next paragraph, were K_T=0.2, K_Q=0.05 and spindle torque = 3 Nm in this example.

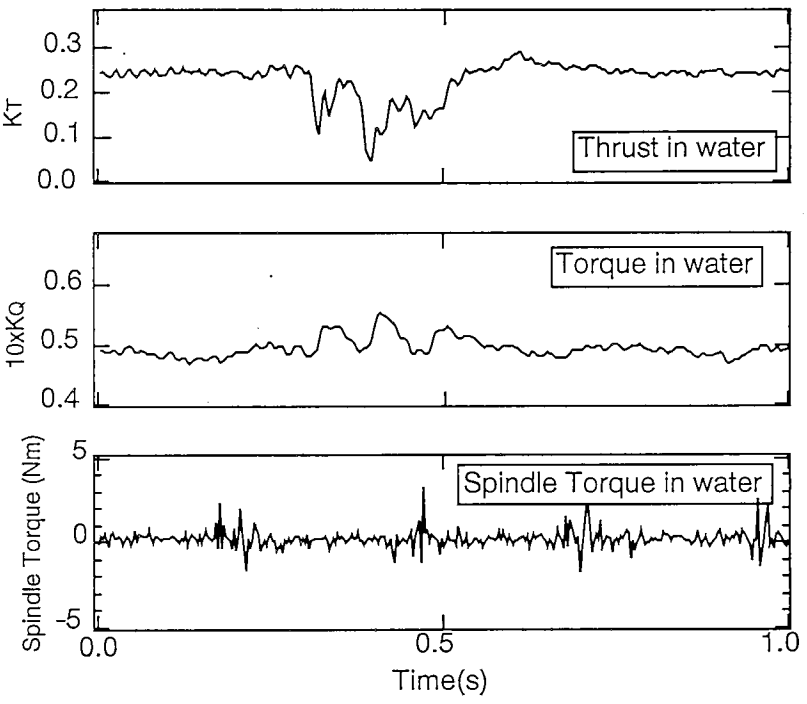

Fig. 9 Time Histories of Samples in Ice Collision Test in Water

Figures 10 and 11 show the variations of thrust and torque peaks determined in such a manner that the mean values without the effect of the blockage were subtracted from the peak values in order to determine the effect of the ice block. The horizontal axis shows ice compressive strength.

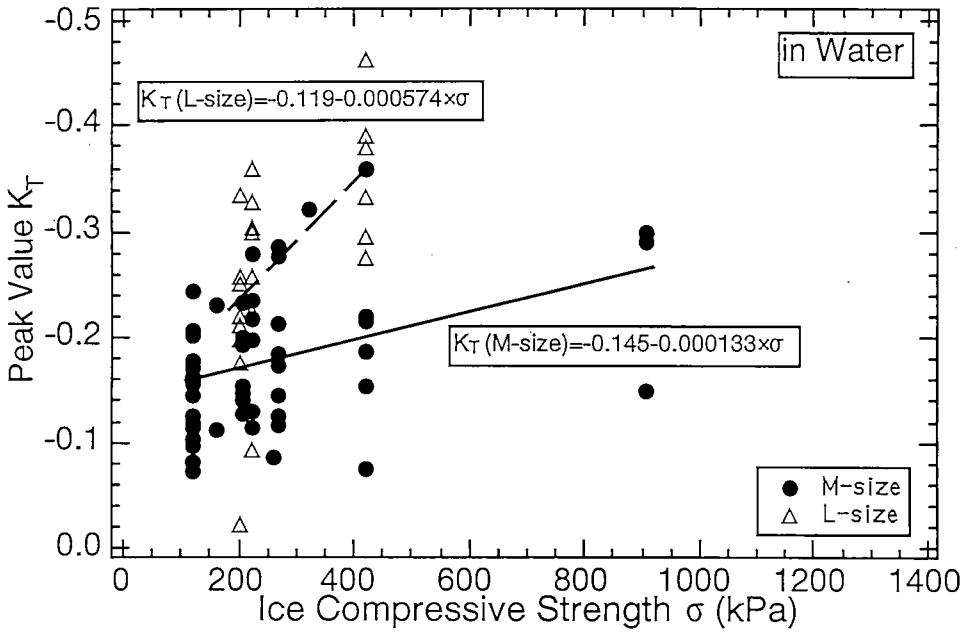

Fig. 10 Variation of K_T Increment with Ice Strength;
Ice Collision Test in Water

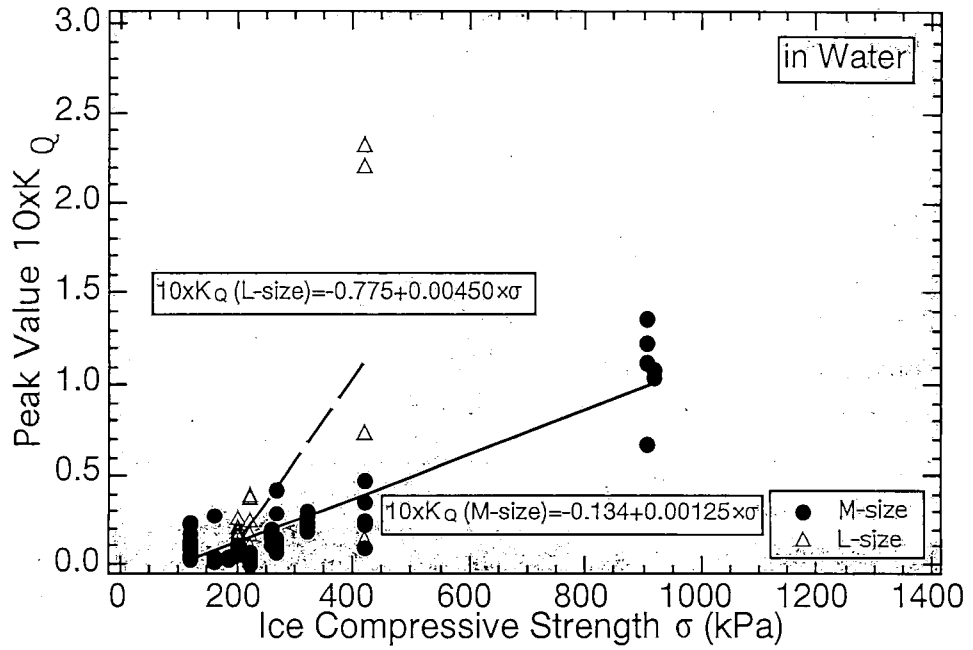

Fig. 11 Variation of K_Q Increment with Ice Strength;
Ice Collision Test in Water

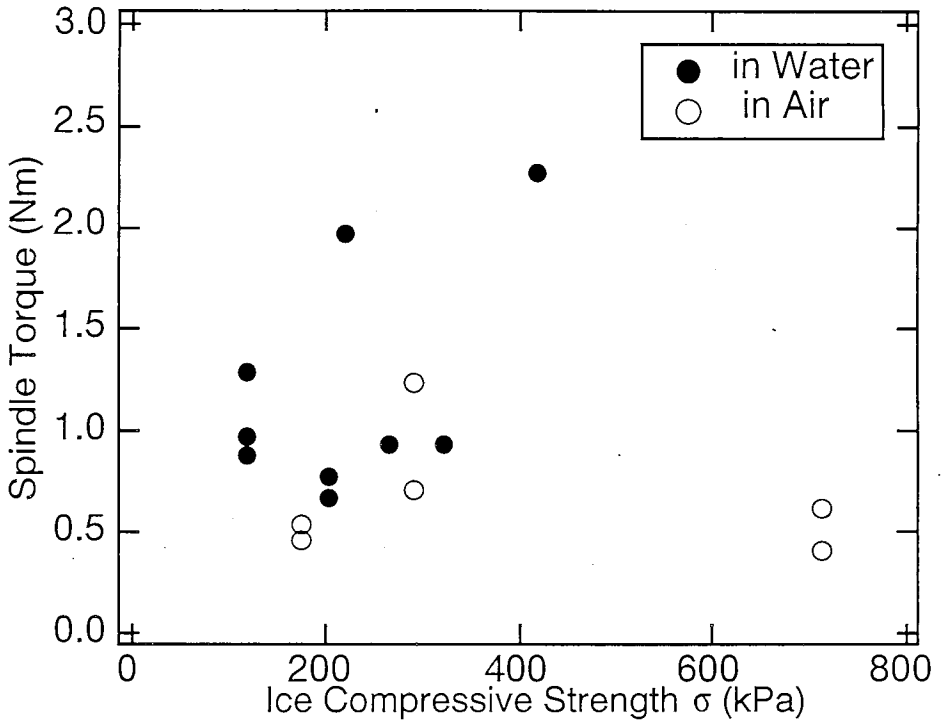

Fig. 12 Variation of Spindle Torque Increment with Ice Strength; Ice Collision Test in Water

Lines in these figures are mean lines. Both K_T and K_Q increase with the ice strength, and torque is much more affected by the ice strength than is thrust. The influence of ice block size is also seen.

Figure 12 shows the change of the spindle torque peak with the variation of ice compressive strength, together with the results of the tests in air. The spindle torque peak also increases as the ice strength increases.

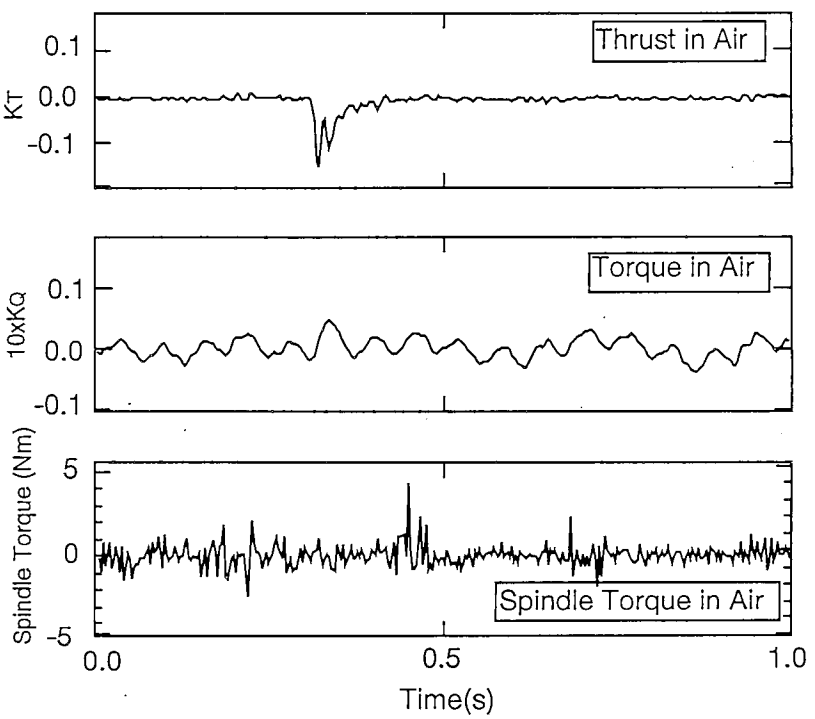

Fig. 13 Time Histories of Samples of Ice Collision Test in Air

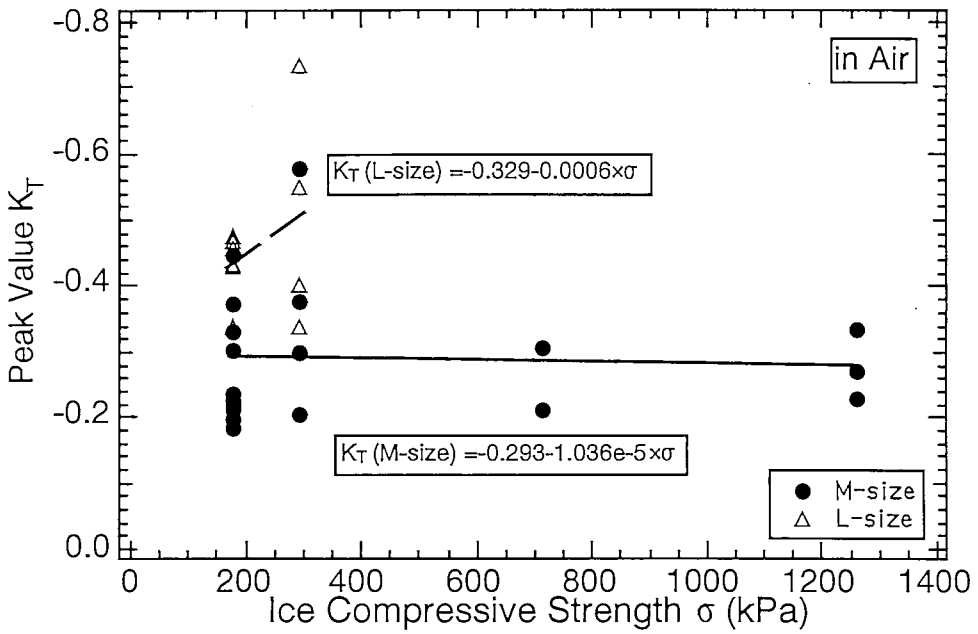

Fig. 14 Variation of K_T Increment with Ice Strength;
Ice Collision Test in Air

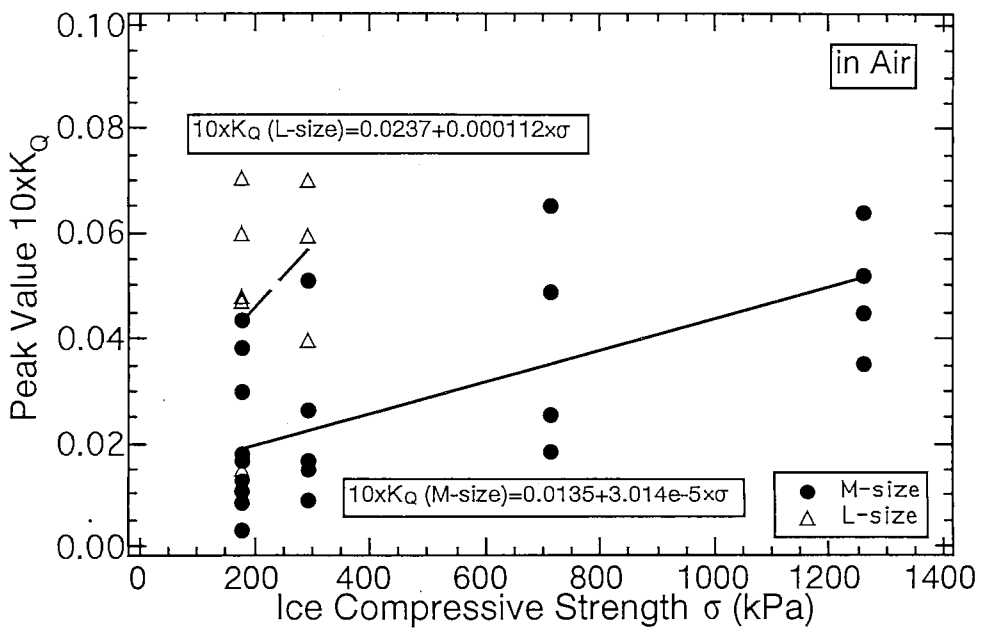

Fig. 15 Variation of K_Q Increment with Ice Strength;
Ice Collision Test in Air

4.2 Ice Block Collision Test in Air

Thirty-seven tests were carried out in air. Figure 13 shows an example of time histories of measured thrust, torque and spindle torque. In this case, an ice block came into contact with the leading edge of blade A. Since no hydrodynamic force acts on the propeller, the peak duration is shorter than that in water shown in Fig. 9. This example shows the peak values of K_T=0.12, K_Q=0.05 and spindle torque = 4 Nm.

Figures 14 and 15 show the variations of K_T and K_Q peaks with ice compressive strength, and correspond to Figs. 10 and 11 in water.

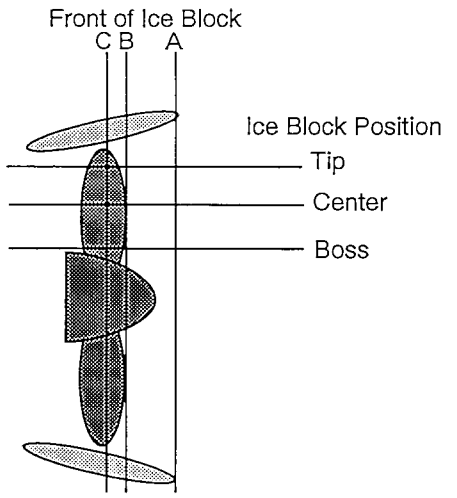

Fig. 16 Block Positions in Ice Blockage Test

4.3 Ice Blockage Test

The purpose of this test is to estimate F_{hydro}, which is the hydrodynamic force due to proximity between the propeller blade and ice block. Eighteen tests were carried out. Figure 16 shows the positions of the ice block. Positions A, B and C in the figure denote the positions of the downstream edge of the ice block. At position A, the downstream edge of the ice block coincides with the upstream edge of the propeller nozzle. At position B, the ice block is located just in front of the propeller, and position C is the most proximate condition. The ice block approached the propeller, was milled, and then stopped at that position. Three positions in the propeller radial direction, Tip, Center and Boss shown in Fig. 16, were tested.

Figures 17 and 18 show the averaged increments of K_T and K_Q due to the presence of the ice block. It is reasonable that the position of C and Tip indicates the highest values. The increment of K_Q is comparable to that of the ice collision tests in water with weak ice, while the increment of K_T is small.

Additional tests with other block positions of Y and Z in Fig. 19 were also performed. The results are shown in Table 4. The increments of K_T and K_Q of the position Z are about 3 times larger than those at the previous position, i.e. C of Figs. 17 and 18. Thus ice blockage, as at Z, can lead to severe hydrodynamic force.

5 SEPARATION OF ICE FORCE INTO COMPONENTS

Based on the results from the experiments mentioned so far, we can estimate the amount of

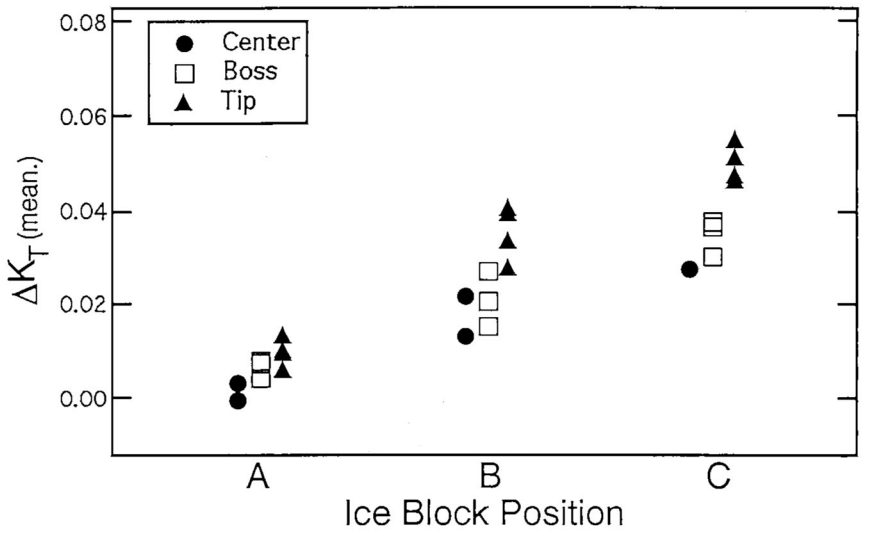

Fig. 17 Effect of Block Position on K_T Increment; Ice Blockage Test

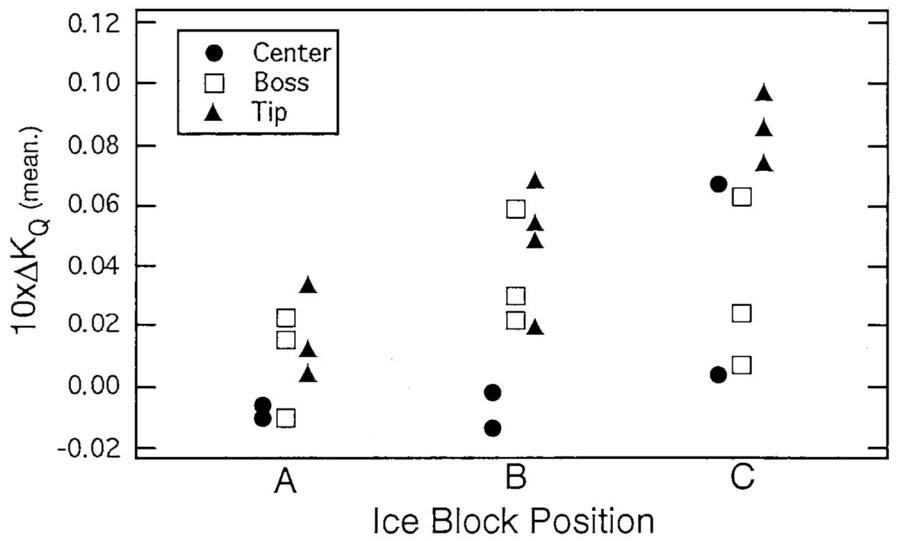

Fig. 18 Effect of Block Position on K_Q Increment; Ice Blockage Test

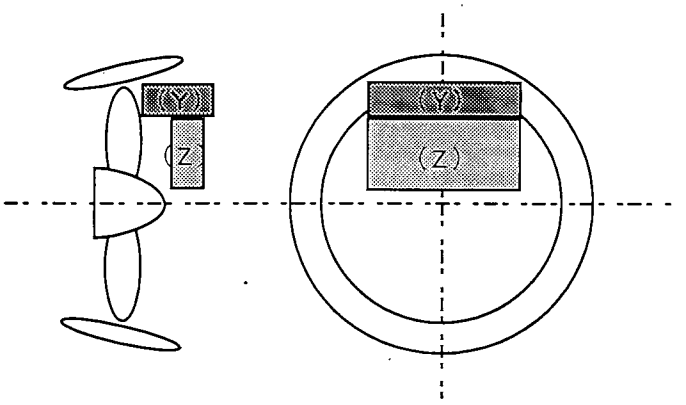

Fig. 19 Block Positions Y and Z in Ice Blockage Test

Table 4 Averaged K_T and K_Q Increments at Block Positions Y and Z

Position	ΔK_T(mean.)	$\Delta 10xK_Q$(mean.)
(Y)	0.0722	0.134
(Z)	0.170	0.311

each force component. From the viewpoint of safety, we should discuss the most severe case in which the maximum ice force occurs. It is the case in which ice collides with the blade tip, since blade speed becomes the maximum at the tip, as the moment at the blade root does, because of the long distance to the loading point. In terms of F_{hydro}, Figs. 17 and 18 indicate K_T=0.050 and $10\times K_Q$=0.088.

Figures 20 and 21 show the variation of ice force when the ice block collided with the tip of the blade in water. The data were extracted from Figs. 10 and 11. Figures 22 and 23 are similar data in air, which were extracted from Figs. 14 and 15. Solid lines in these figures are mean lines. Taking scatter of data into account, we defined the maximum force as shown by the broken lines in Figs. 20 - 23. The lines envelop the data and have the same inclination as the mean lines. In future these lines should be determined statistically by making more tests.

Figures 20 through 23 show that the inclinations of lines of maximum force for the tests in air are less than those for the tests in water. This means that $F_{inertia2}$, the added mass force, changes greatly with the ice strength. However, this conclusion is questionable since ice motion showed negligible dependence on ice strength, as mentioned previously. A more probable conclusion is that the behavior of ice failure in air was affected more by the ice strength than when it was in water. In water, the ice failed in a similar manner regardless of the ice strength since the water provided resistance to ice motion. In air, some of the ice blocks with high

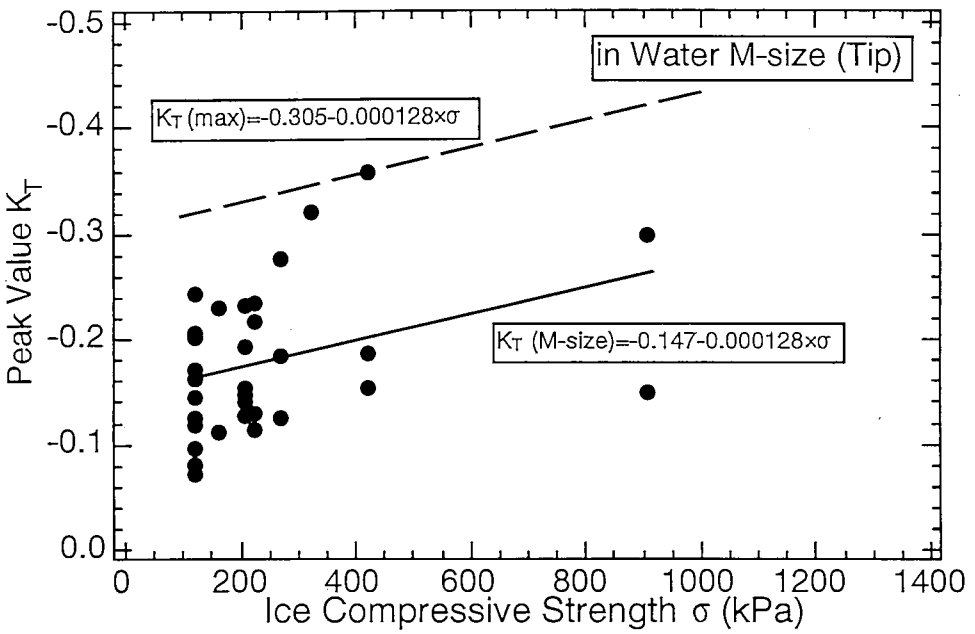

Fig. 20 Variation of K_T Increment with Ice Strength;
Contact with Blade Tip, Ice Collision Test in Water

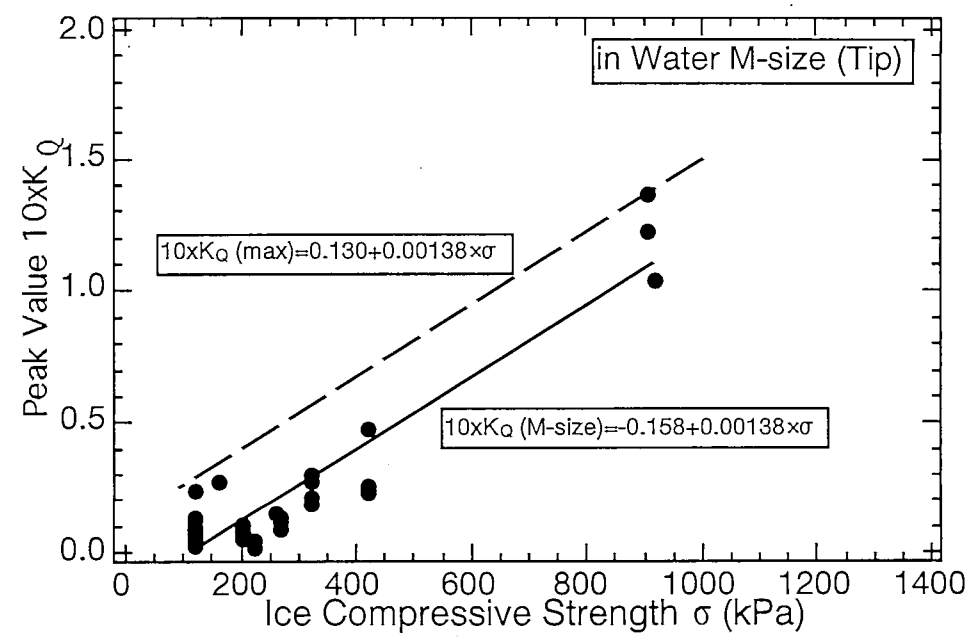

Fig. 21 Variation of K_Q Increment with Ice Strength;
Contact with Blade Tip, Ice Collision Test in Water

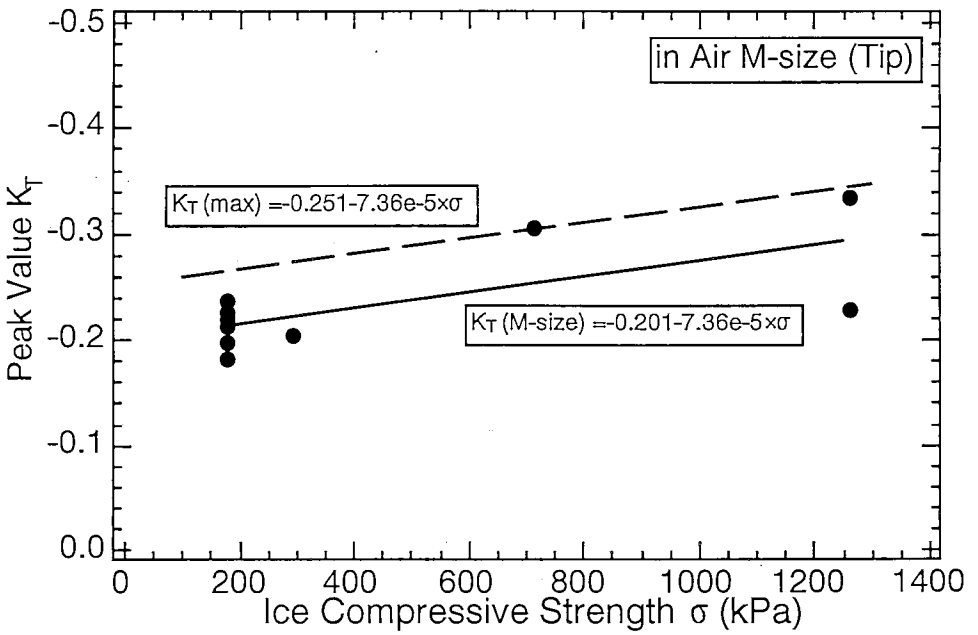

Fig. 22 Variation of K_T Increment with Ice Strength;
Contact with Blade Tip, Ice Collision Test in Air

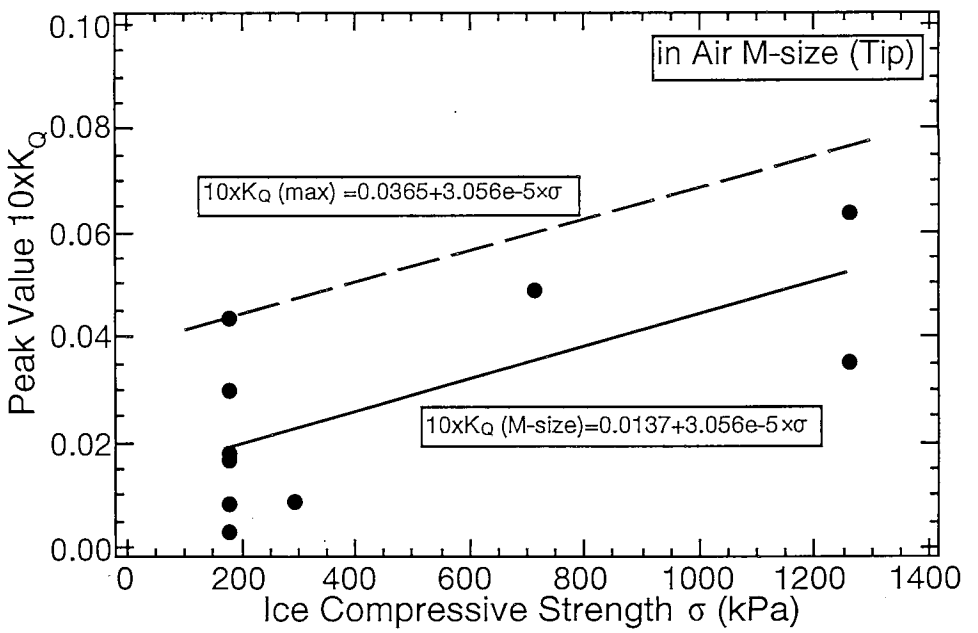

Fig. 23 Variation of K_Q Increment with Ice Strength;
Contact with Blade Tip, Ice Collision Test in Air

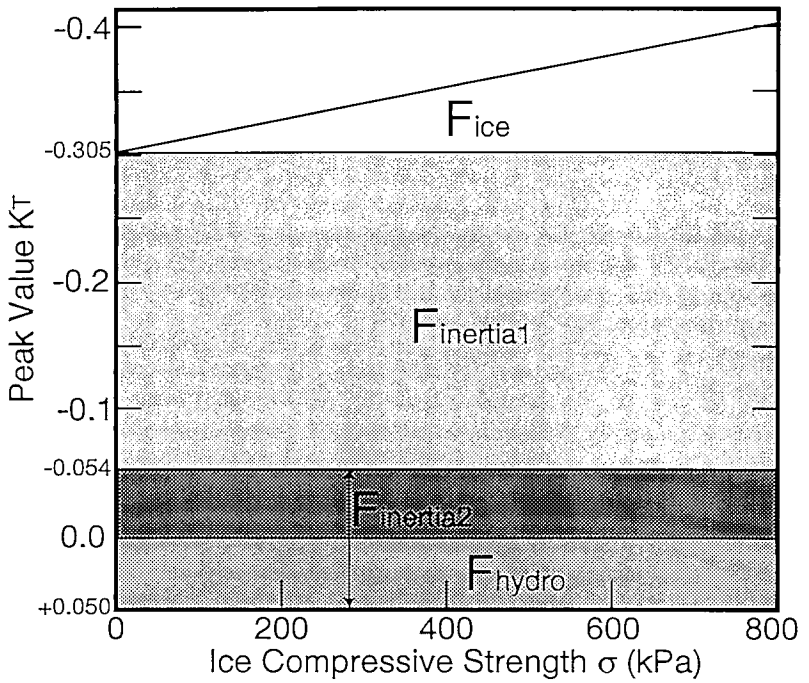

Fig. 24 Ice Load Components in K_T

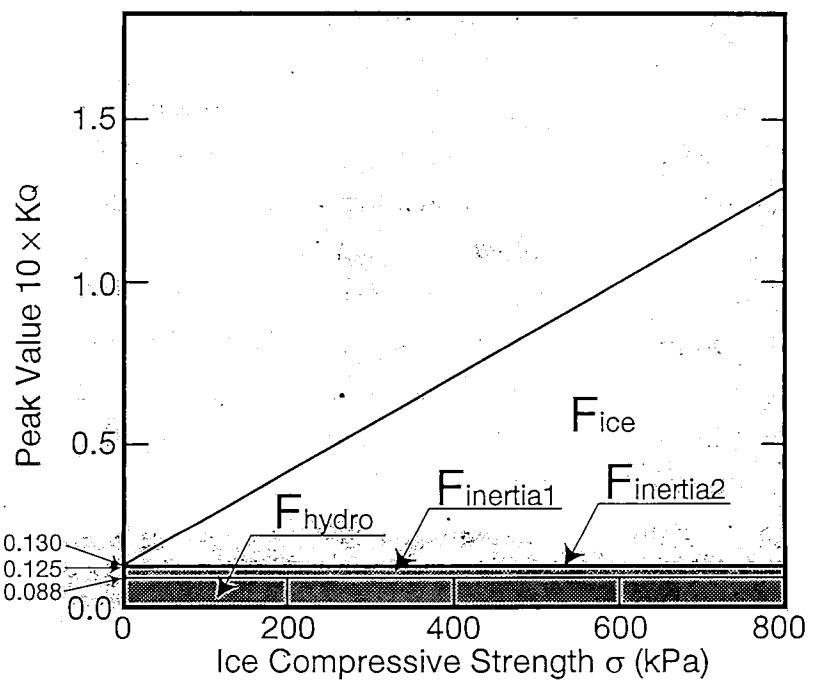

Fig. 25 Ice Load Components in K_Q

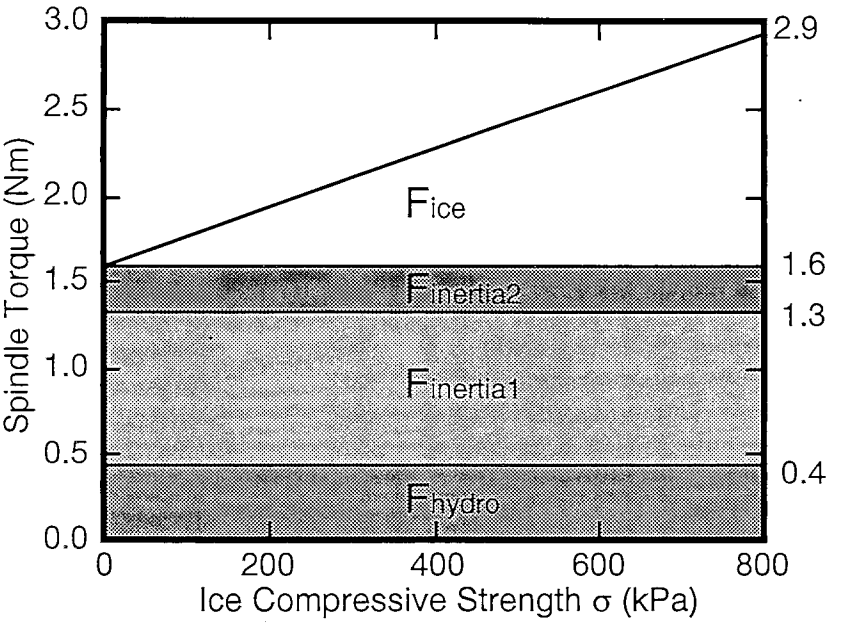

Fig. 26 Ice Load Components in Spindle Torque

strength were hit away by the blade, so only part of the block was damaged with cracks. In such a case, F_{ice} is lower than that of ice failure in water. Thus $F_{inertia1}$ and $F_{inertia2}$ are assumed to be constant to a first approximation, as mentioned previously, and $F_{inertia1}$ is determined to be the force at ice strength = 0, from the tests in air: $K_T = 0.251$ from Fig. 22 and $10 \times K_Q = 0.0365$ from Fig. 23.

The force at ice strength = 0 from the test in water is regarded to be $F_{hydro}+F_{inertia1}+F_{inertia2}$, which is not affected by the ice strength. The rest of the ice load is determined to be F_{ice}, which is assumed to be proportional to the ice strength. Figures 24 and 25 show the results of the decomposition of thrust and torque, respectively. Figure 24 indicates that the largest component is inertia force, $F_{inertia1}$, and the ice strength dependence of F_{ice} is small. This is because the ice blocks collided with the propeller with some momentum and ice milling was rare. Figure 25 shows that F_{ice} is highly dependent on the ice strength and is the largest of all the force components. This is because the direction of the ice failure force is close to the propeller rotation direction, resulting in a more significant effect on torque.

A similar decomposition procedure was also applied to spindle torque data although the amount of data is limited. Figure 26 shows the result, where the effects of each force component are between those on propeller thrust and torque.

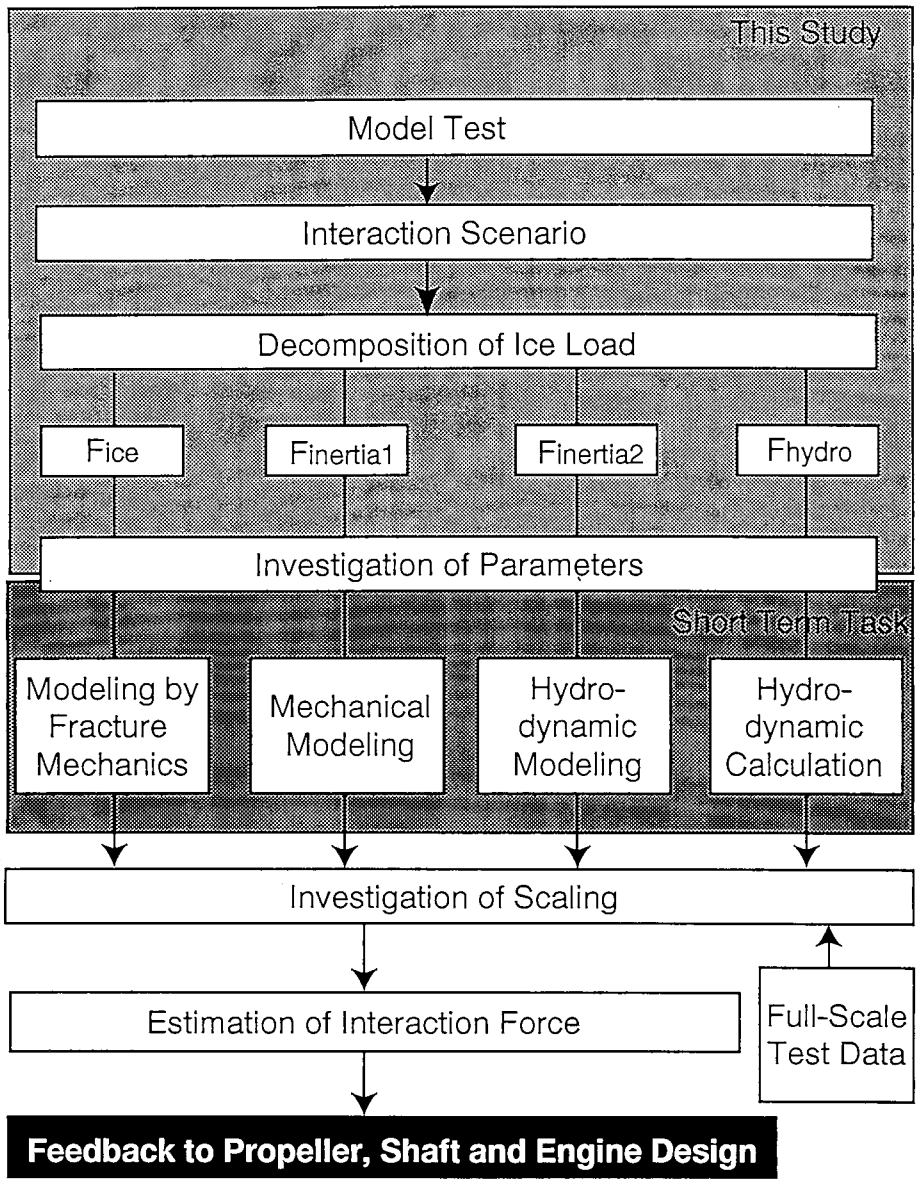

Fig. 27 Flow Chart for Feedback of the Present Study to the Design Work

6 FUTURE WORK

As described previously, we have succeeded in dividing the ice-propeller interaction force into 4 components, i.e., F_{ice} (ice failure force), $F_{inertia1}$ (ice mass force), $F_{inertia2}$ (added mass force) and F_{hydro} (hydrodynamic force due to proximity). Such an approach is a promising way to clarify the complicated ice-propeller interaction phenomenon and to establish a method to predict the full-scale interaction forces precisely.

In this paper, maximum lines of ice force were determined in such a way that the lines passed through the maximum values, but these lines should be determined in a statistical manner

Table 5 Future Tasks

•Short-Term Task •Survey of literature (focus on modeling) •Modeling of This Propeller •Supplement Experiment (Changing Propeller Revolution, Using Small Propeller) •Completion of Modeling of This Propeller
•Long-Term Task •Modeling of General Propeller •Hydrodynamic Analisys by Numerical •Actual Ship Tests •Modeling with a General Scaling Method •Completion of Modeling of General Propeller

by performing more tests. Discussion on scaling factors such as propeller diameter, revolution speed, ice strength and flow speed is also an important future task. Figure 27 shows the scope of this study and what has been done up to now. In the present study, we demonstrated that our proposed scenario of ice-propeller interaction is correct, and the experimental decomposition method proposed in this report is valid. At the next stage, the modeling of each process should be accomplished through discussions on the major parameters involved. Then the modeling should be verified and improved through rational scaling and comparison with full-scale data. Table 5 shows the items to be accomplished to complete the flow chart in Fig. 27.

7 CONCLUDING REMARKS

This study began with the premise that ice-propeller interaction force was divided into 4 components. An experimental method was proposed to extract these components on the basis of physical considerations and using high-speed video observations. The components were (1) force due to ice failure, (2) force due to momentum change of the ice block, (3) force due to the added mass of ice and (4) hydrodynamic force due to the proximity of the ice block to the

propeller blade.

Tests were performed for a nozzle propeller model of a 267mm-diameter propeller. The experiments to separate the force components were (1) ice block collision tests in water with various ice strengths, (2) ice block collision tests in air with various ice strengths and (3) ice blockage tests where the ice block was fixed in front of propeller. Those tests enabled decomposition of the ice-propeller interaction force into the 4 components noted above. The following results, which revealed that force components other than ice failure force were also significant, were obtained.

1. The ice failure force component seems to be proportional to the ice strength.
2. For the thrust, the inertia force is by far the major component and the ice failure force is minor. The hydrodynamic force increases the thrust, while the other forces decrease it.
3. For the torque, the ice failure force is strongly dependent on the ice strength and is the largest of all the force components, followed by the hydrodynamic force and then the inertia force which is about half the hydrodynamic force.
4. For the spindle torque, the inertia force and the ice failure force are the largest components and are comparable to each other. Hydrodynamic force is approximately half the inertia force.

As mentioned above, inertia and hydrodynamic forces are comparable to or larger than the ice failure force, as far as a nozzle propeller is concerned. Rational scaling laws should be considered and applied to the respective force components when ice force on a full-scale propeller is extrapolated from the results of the model experiment.

8 ACKNOWLEDGMENT

A part of this study was carried out in the course of the NSR Research Panel in Japan (JANSROP). Financial support from SHIP & OCEAN FOUNDATION and The Nippon Foundation is acknowledged. The authors are grateful to Professor Yuzuru Fujita, Professor Emeritus of the University of Tokyo, for leading the Panel as the chairman of the Steering Committee of the Panel. They would also like to thank Professor Hiromitsu Kitagawa, Hokkaido University for his valuable comments and suggestions to this study.

9 REFERENCES

Bose, N., 1995, "Ice Blocked Propeller Performance Prediction Using Panel Method," OERC Report No. TR-HYD-95006, Memorial University of Newfoundland, Canada, 31p. + 13 figures.

Fleet Technology Ltd., 1992, "Research on Ice/Propeller Interaction," Report Submitted to the Institute for Marine Dynamics, National Research Council of Canada.

Ishikawa, S., and Kawasaki, S., 1996, "A Series of Model Tests in Ice of Ice-Going Cargo Ships for Future Traffic in the Northern Sea Route," Northern Sea Route; Future and Perspective (Proc. INSROP Symp. Tokyo 1995), Ship & Ocean Foundation, Japan, pp.469-474.

Izumiyama, K., and Uto S., 1996, "Ice Resistance of Three Bow Forms for the NSR Cargo Ship," Northern Sea Route; Future and Perspective (Proc. INSROP Symp. Tokyo 1995), Ship & Ocean Foundation, Japan, pp.459-467.

Jagodkin, V. Y., 1963, "Analytical Determination of the Resistance Moment of a Propeller during Its Interaction with Ice,"(trans.) Problems of the Arctic and Antarctic, vol.13, pp.121-127.

Jussila, M., and Soininen, H., 1991, "Interaction between Ice and Propeller," Research Notes 1281, Technical Research Centre of Finland.

Kishi, S., and Narita, S., 1996, "Development of Optimum Hull Forms for Icebreaking Cargo Ships for the Northern Sea Route," Northern Sea Route; Future and Perspective (Proc. INSROP Symp. Tokyo 1995), Ship & Ocean Foundation, Japan, pp.475-482.

Kitagawa, H., 1996, "R&D Project of a Cargo Ship for the NSR," Northern Sea Route; Future and Perspective (Proc. INSROP Symp. Tokyo 1995), Ship & Ocean Foundation, Japan, pp.453-457.

Koskinen, P., Jussila, M., and Soininen, H., 1996, "Propeller ice load models," VTT Research Notes 1739, Technical Research Centre of Finland.

Shih, L. Y., and Zheng, Y., 1992, "Constricted Hydrodynamic Flow due to Proximate Ice Blockage over a Blade Profile in Two Dimension," Proc. 2nd Symp. Propellers and Cavitation, Hangzou, China, CSNAME, pp. 74-79.

Soininen, H., and Veitch, B. (ed.), 1996, "Propeller-Ice Interaction, Joint research project arrangement #6, (JRPA #6), Joint conclusion report," VTT Research Notes 1762, Technical Research Centre of Finland, NRC Report IR-1996-06, Institute for Marine Dynamics, National Research Council of Canada.

Tamura, K., and Yamaguchi, H., 1996, "An Attempt to Draw a Scenario of Ice/Propeller Interaction," Northern Sea Route; Future and Perspective (Proc. INSROP Symp. Tokyo 1995), Ship & Ocean Foundation, Japan, pp.491-496.

Veitch, B., 1995, "Predictions of Ice Contact Forces on a Marine Screw Propeller during the Propeller-Ice Cutting Process," Mechanical Engineering Series No.118, Acta Polytechnica Scandinavica.

Veitch, B., Meade, C., Bose, N., and Liu, P. F., 1997, "Predictions of Hydrodynamic and Ice Contact Loads on Ice-Class Screw Propellers," Proc. 16th Intern. Conf. Offshore Mechanics and Arctic Engineering (OMAE) / 14th Intern. Conf. Port and Ocean Engineering in Arctic Conditions (POAC), Yokohama, 1997 OMAE - Vol. IV, ASME, pp.119-125.

Walker, D., Bose, N., and Yamaguchi, H., 1994, "Hydrodynamic Performance and Cavitation of an Open Propeller in a Simulated Ice-Blocked Flow," Journal of OMAE, Vol.116, pp.185-189.

Walker, D., and Bose, N., 1994, "Hydrodynamic Loads and Dynamic Effects of Cavitation on Ice Class Propellers in Simulated Ice Blocked Flows," Proc. SNAME Propellers/Shafting '94 Symp., Virginia Beach, Paper No.20, 19 p.

Walker, D., Bose, N., Yamaguchi, H., and Jones, S., 1997, "Hydrodynamic Loads on Ice Class Propellers During Propeller Ice Interaction," Journal of Marine Science and Technology, The Society of Naval Architects of Japan, Vol.2, No.1, pp.12-20.

REVIEW & DISCUSSION

by Dr. Stephen J. Jones and Dr. Brian Veitch, Institute for Marine Dynamics, National Research Council, Canada.

The authors have devised an experimental program that aims physically to separate into components the forces acting on a nozzled propeller during propeller-ice interaction. The experiments have been carefully planned and the results should be of interest and value to those involved in this particular field of ice navigation.
A discussion of several points raised by the paper is presented following.

1. The title is not accurate. This paper deals with more than hydrodynamic issues.

2. The experimental program that the authors have reported should provide insight into the physical problem of propeller-ice interaction. The proposition that the components can be physically separated and then superimposed can be debated. Loads on the propeller derive from two sources: a) hydrodynamic and b) ice contact. The ice contact load depends on the nature of the contact and ice failure mechanics, and on the geometry and kinematics of the propeller-ice contact. These latter depend on the ice motion, which is governed by the dynamics of the ice. The forces on the ice are buoyancy, drag (and lift), added mass force and added moment of inertia, and contact force. It could be argued that by testing the components separately, the dependencies are lost.

3. When the authors continue this investigation, they should be aware of other recently published work in this area. For example, in section 2 of the paper, the authors say that very few studies have taken account of inertia effects. These effects are dealt with in detail by Veitch (1995) using classical rigid body dynamics, and also Koskinen et al. (1996). Both of these works also include experimental studies on the mechanics of ice failure during propeller-ice interaction. Further, Bose (1996) has recently developed a panel method for analyzing the hydrodynamic loads on a propeller in a blocked flow, and Walker (1994) has reported cavitation tunnel tests of propellers in blocked flow.

4. The authors claim in section 3 that the contact point during propeller ice interaction tests can be determined from high speed video records. It may be possible to estimate the contact point area from video, but only approximately. Conclusions based on this claim should be qualified.

5. The results of the ice block collision tests in water (section 4.1) are very interesting. The time histories look quite qualitatively realistic. Shaft dynamics does not appear to have been a problem. I question the claim that shaft thrust and blade spindle torque peaks appeared before and after, respectively, the direct contact. (see comment 4).

6. The results of ice block collision tests in air (section 4.2) show that the width of the peak plotted force (thrust in air) is smaller in air than in water. A possible explanation for this difference is that, in the absence of water, the ice is hit by only one blade, whereas in water the ice is hit by 2 or 3 consecutive blades.

7. The results of the ice blockage tests in water (section 4.3) are very interesting indeed.

8. With reference to the discussion in section 5, it can be expected that the higher strength ice will be more rapidly accelerated when impacted by the blade. This would lead to a higher added mass force.

In conclusion, the authors are to be commended for this novel experimental approach and the results. It is the hope of the reviewers that the discussion offered here will be of some use as the authors continue their investigation.

Additional references

Walker, D. 1994. Hydrodynamic loads and dynamic effects of cavitation on ice class propellers in simulated ice blocked flow. *Proceedings Propeller/Shafting '94*, Virginia Beach, paper No.20, 19 pages.

Bose, N. 1996. Ice blocked propeller performance using a panel method. To appear in *Trans. Royal Institution of Naval Architects.*

Veitch, B. 1995. Predictions of ice contact forces on a marine screw propeller during the propeller-ice cutting process. *Acta Polytechnica Scandinavia*, Mechanical Engineering Series No. 188, The Finnish Academy of Technology, Helsinki, 140 pp.

Koskinen, P., Jussila, M., and Soininen, H. 1996, Propeller ice load models. VTT *Research Notes* 1739, Technical Research Centre of Finland, 82 pp.

AUTHORS' REPLY

We express our sincere gratitude to the reviewers for their invaluable suggestions and comments. Since we have already revised the report in accordance with their comments, their discussions have already been answered in the contents of the report. Here we hope to add some details.

1. Only the hydrodynamic aspect of the present study was dealt with in the INSROP Project I.I.9. The other parts of the study were carried out under a domestic joint research project under SHIP & OCEAN FOUNDATION with subsidy of The Nippon Foundation. When we drafted the paper, we preferred the completeness of the contents to describing only the part obtained from the INSROP Project. This was the reason for the unbalance between the original title and the contents. After talking with the INSROP Secretariat, we decided to modify the title into the present one to express the contents properly.

2. Our final goal is to provide rational scaling laws for the estimation of fullscale propeller load from the model tests as shown in Fig. 27. As the first step, we assumed the decomposition of the load. There would be a case where the interaction among the load components is not negligible, but as far as the present experiment is concerned, we think the interaction was not significant.

3. Thank you for reminding us the recent works. Certainly these works were not referred in the draft of the report. They are cited in this report.

4. Since the propeller revolution rate is 4 rps and the speed of the high-speed video is 240 frames/s, the propeller blade rotates 6 deg. every frame, which was not too rough resolution to determine the contact point.

5. Although we can't answer this question clearly, possible explanation is as follows. Thrust due to ice-propeller interaction is attributed to the momentum change of the ice block in the propeller axis direction. Torque is due to the ice crushing after the blade has penetrated the ice block to some extent. Since the ice block collides with the propeller blade in propeller axial direction, the thrust peak appears first, followed by the torque peak. For the spindle torque, negative torque appears in the beginning of the collision, since the ice block colliding with the leading edge of the blade gives the momentum in the propeller axis direction. Then positive peak appears after the blade penetrates the ice block well. This is the reason why the spindle torque positive peak appears last.

6. Reviewers' comment is correct.

8. We observed the high-speed video images for 92 collisions in water and 37 collisions in air. As a result, we did not observe any significant effect of ice strength in the ice motion. Therefore, as far as the present experiment is concerned, we concluded that ice mass force and added mass force can be assumed to be independent of ice strength.

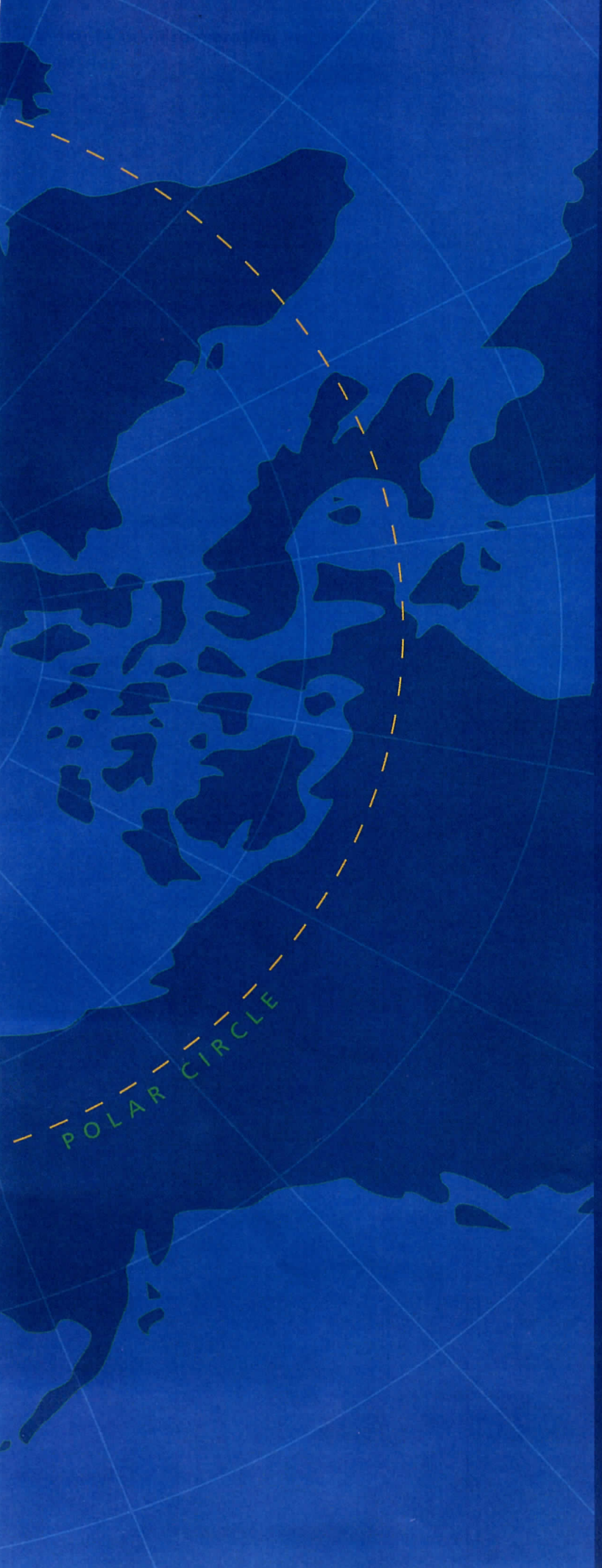

The three main cooperating institutions of INSROP

Ship & Ocean Foundation (SOF), Tokyo, Japan.

SOF was established in 1975 as a non-profit organization to advance modernization and rationalization of Japan's shipbuilding and related industries, and to give assistance to non-profit organizations associated with these industries. SOF is provided with operation funds by the Sasakawa Foundation, the world's largest foundation operated with revenue from motorboat racing. An integral part of SOF, the Tsukuba Institute, carries out experimental research into ocean environment protection and ocean development.

Central Marine Research & Design Institute (CNIIMF), St. Petersburg, Russia.

CNIIMF was founded in 1929. The institute's research focus is applied and technological with four main goals: the improvment of merchant fleet efficiency; shipping safety; technical development of the merchant fleet; and design support for future fleet development. CNIIMF was a Russian state institution up to 1993, when it was converted into a stock-holding company.

The Fridtjof Nansen Institute (FNI), Lysaker, Norway.

FNI was founded in 1958 and is based at Polhøgda, the home of Fridtjof Nansen, famous Norwegian polar explorer, scientist, humanist and statesman. The institute spesializes in applied social science research, with special focus on international resource and environmental management. In addition to INSROP, the research is organized in six integrated programmes. Typical of FNI research is a multi-disciplinary approach, entailing extensive cooperation with other research institutions both at home and abroad. The INSROP Secretariat is located at FNI.